Myogenic Vasoconstriction Requires Canonical $G_{q/11}$ Signaling of the Angiotensin II Type 1a Receptor in the Murine Vasculature

Yingqiu Cui[1], Mario Kassmann[1], Sophie Nickel[1], Chenglin Zhang[2], Natalia Alenina[3,4], Yoland Marie Anistan[1], Johanna Schleifenbaum[1], Michael Bader[3,4,5,6], Donald G. Welsh[7], Yu Huang[2], Maik Gollasch[1,8,9]

1. Charité - Universitätsmedizin Berlin, Experimental and Clinical Research Center (ECRC), a joint cooperation between the Charité Medical Faculty and the Max Delbrück Center for Molecular Medicine (MDC), Lindenberger Weg 80, 13125 Berlin, Germany,
2. Heart and Vascular Institute and School of Biomedical Sciences, Chinese University of Hong Kong, Hong Kong, China,
3. Max Delbrück Center for Molecular Medicine, Berlin, Germany,
4. DZHK (German Center for Cardiovascular Research), Partner Site Berlin, Berlin, Germany.
5. Charité – Universitätsmedizin Berlin, Germany.
6. Institute for Biology, University of Lübeck, Lübeck, Germany.
7. Robarts, Research Institute, Department of Physiology and Pharmacology, Western University, London, ON, Canada,
8. Charité - Universitätsmedizin Berlin, Medical Clinic for Nephrology and Internal Intensive Care, Campus Virchow, 13353 Berlin, Germany,
9. Department of Internal Medicine and Geriatrics, University Medicine Greifswald, Greifswald, Germany

Corresponding author: Maik Gollasch, Experimental and Clinical Research Center (ECRC), 13125 Berlin Germany. E-mail: maik.gollasch@charite.de

Key Words: Angiotensin II type 1a receptor, biased ligands, myogenic vasoconstriction, arterial smooth muscle

31   **Abstract**

32   **Background:** The myogenic response is an inherent vasoconstrictive property of resistance

33   arteries to keep blood flow constant in response to increases in intravascular pressure.

34   Angiotensin II (Ang II) type 1 receptors (AT1R) are broadly distributed, mechanoactivated

35   receptors, which have been proposed to transduce myogenic vasoconstriction. However, the

36   AT1R subtype(s) involved and their downstream G protein- and β-arrestin-mediated signaling

37   pathways are still elusive. **Objective:** To characterize the function of AT1aR and AT1bR in

38   the regulation of the myogenic response of resistance size arteries and possible downstream

39   signaling cascades mediated by $G_{q/11}$ and/or β-arrestins. **Methods:** We used $Agtr1a^{-/-}$,

40   $Agtr1b^{-/-}$ and tamoxifen-inducible smooth muscle-specific AT1aR knockout mice (SM-$Agtr1a$

41   mice). FR900359, [Sar1, Ile4, Ile8] Ang II (SII) and TRV120055 were used as selective $G_{q/11}$

42   protein inhibitor and biased agonists to activate non-canonical β-arrestin and canonical $G_{q/11}$

43   signaling of the AT1R, respectively. **Results:** Myogenic and Ang II-induced vasoconstrictions

44   were diminished in the perfused renal vasculature of $Agtr1a^{-/-}$ and SM-$Agtr1a$ mice. Similar

45   results were observed in isolated pressurized mesenteric and cerebral arteries. Myogenic

46   tone and Ang II- induced vasoconstrictions were normal in arteries from $Agtr1b^{-/-}$ mice. The

47   $G_{q/11}$ blocker FR900359 decreased myogenic tone and Ang II vasoconstrictions while

48   selective biased targeting of AT1R β-arrestin signaling pathways had no effects. **Conclusion:**

49   The present study demonstrates that myogenic arterial constriction requires $G_{q/11}$-dependent

50   signaling pathways of mechanoactivated AT1aR but not G protein-independent, noncanonical

51   alternative signaling pathways in the murine mesenteric, cerebral and renal circulation.

52   **1. Introduction**

53   Myogenic vasoconstriction reflects the inherent ability of resistance arteries to adapt their

54   diameter in response to alterations of intraluminal pressure. This response was first described

55   by William Bayliss (2) and it reflects changes to the contractile state of vascular smooth

56   muscle.   Increases in transmural pressure cause vasoconstriction whereas decreases

57   produce the opposing effect; this prototype of autoregulation has been observed in various

58   microvascular arterial beds (8) and it is responsible for maintaining constant blood flow during

59   fluctuations in perfusion pressure. Many cardiovascular disorders are associated with

60   dysfunctional arterial myogenic response and they include hypertension, chronic heart failure,

61   ischemic stroke, diabetes mellitus (6) (14) (31) (41) (45). Despite the functional importance of

62   the myogenic response, the molecular mechanisms responsible for sensing intraluminal

63   pressure has yet to be fully clarified.

64   Myogenic vasoconstriction is mediated by pressure-dependent depolarization of vascular

65   smooth muscle cells, an event that augments Ca^{2+} influx through voltage-dependent $Ca_v1.2$

66   channels (39) (7) (9) (16) (17) (38). $G_{q/11}$-coupled receptors (GPCRs) are thought to function

67   as the upstream sensor of membrane stretch (37), with angiotensin II type 1a ($AT_{1a}R$), and

68   perhaps AT1bR receptors in concert with cysteinyl leukotriene 1 receptor ($CysLT_1R$), playing

69   a particularly important role in the mesenteric and renal circulation (3) (40) (46) (49). AT1Rs

70   are known to couple primarily to classical $G_{q/11}$ proteins to activate multiple downstream

71   signals, including protein kinase (PKC), extracellular signal-regulated kinases (ERK1/2), Raf

72   kinases, tyrosine kinases, receptor tyrosine kinases (EGFR, PDGF, insulin receptor) and

73   reactive   oxygen   species   (ROS)   (1).   The   AT1R   activation   also   stimulates   G

74   protein-independent signaling pathways such as β-arrestin-mediated mitogen-activated

75   protein kinase (MAPK) activation and Src-JAK/STAT (1). Recently, it has been shown that the

76   activation of intracellular signaling by mechanical stretch of the AT1R does not require the

77   natural ligand angiotensin II (Ang II) (44) (55) (46) but requires the activation of the transducer

78   ß-arrestin (44). Interestingly, mechanical stretch appears to allosterically stabilize specific

79   β-arrestin-biased active conformations of AT1R to promote noncanonical downstream

80   signaling mediated exclusively by the multifunctional scaffold protein, β-arrestin (50).

81   Whether this noncanonical ß-arrestin effector pathway plays a role in myogenic and

82   ligand-dependent vasoconstriction has yet to be ascertained.

83   This study explored the specific function of AT1R subtypes in the regulation of myogenic

84   tone and whether downstream signaling pathways are dependent on canonical $G_{q/11}$ and/or

85   noncanonical alternative signaling pathways. In this regard, we generated mice with cell

86   specific deletion of smooth muscle AT1a receptors (SM-*Agtr1a* mice) and studied the effects

87   of biased GPCR agonists and $G_{q/11}$ protein inhibition on tone development in three distinct

88   vascular beds (renal, cerebral and mesenteric circulation). We found that the AT1aR coupled

89   towards the canonical $G_{q/11}$ signaling pathway is required for the myogenic response in all

90   three   vascular   beds.   Our   data   argue   against   involvement   of   noncanonical   G

91   protein-independent alternative signaling downstream of the AT1aR to cause myogenic

92   vasoconstriction.

2. Materials and Methods

2.1 Mouse Model

95   We used the SMMHC-Cre-ER^{T2} transgenic mouse line expressing Cre recombinase in

96   smooth muscle cells under control of the smooth muscle myosin heavy chain promoter (26)

97   and a mouse line bearing a floxed allele of the *Agtr1a* gene (*Agtr1a*^flox^), encoding the major

98   murine AT1 receptor isoform (AT1aR) (48) to generate SMMHC-Cre+*Agtr1a*^flox/flox^

99   (SM-*Agtr1a*^-/-^) mice (**Figure 1A**). Genotyping was performed by polymerase chain reaction

100 (PCR) analysis of tail DNA as described previously (26). Amplification of the SMMHC-Cre

101 gene was performed in a multiplex PCR with the primers TGA CCC CAT CTC TTC ACT CC

102 (SMWT1), AAC TCC ACG ACC ACC TCA TC (SMWT2), and AGT CCC TCA CAT CCT CAG

103 GTT (phCREAS1) (13). The following primers (5'-3') were used to identify *Agtr1a*^flox^ alleles:

104 forward GCT TTC TCT GTT ATG CAG TCT, reverse ATC AGC ACA TCC AGG AAT G. Adult

105 (12-16 weeks) male mice were injected with tamoxifen (30 µg/mg body weight) on 5

106 consecutive days. Isolated arteries were usually obtained after 2 to 3 days after tamoxifen

107 treatment. **Figure 1B** shows reduction of AT1aR expression in vascular smooth muscle cells

108 of SM-*Agtr1a*^-/-^ arteries. We also studied adult (12-16 weeks) male mice with global AT1a

109 receptor deficiency (*Agtr1a*^-/-^) (24) (46) (25), and with global AT1b receptor deficiency

110 (*Agtr1b*^-/-^) (40). Age-matched male mice were used as controls in the experiments. Animal

111 care followed American Physiological Society guidelines, and all protocols were approved by

112 local authority (LAGeSo, Berlin, Germany) and the animal welfare officers of the Max

113 Delbruck Center for Molecular Medicine. Mice were maintained in the Max Delbrück Center

114 animal facility in individually ventilated cages (Tecniplast, Deutschland) under standardized

115 conditions with an artificial 12-hour dark-light cycle, with free access to standard chow (0.25%

116 sodium; SSNIFF Spezialitäten, Soest, Germany) and drinking water. Animals were randomly

117 assigned to the experimental procedures.

118 **2.2 Materials**

119 Antibody to α-smooth muscle actin (α-SMA, #ab8211) was from Abcam (Cambridge, MA,

120 USA). Anti-AT1R (#PA5-20812) and donkey anti-rabbit IgG (H+L) secondary antibody

121 (A10040) were purchased from Thermo Fisher Scientific (Waltham, MA, USA).

122 4',6-diamidino-2-phenylindole (DAPI, #D9542) was purchased from Sigma-Aldrich Co. (St.

123 Louis, MO, USA). Ang II (#A9525), SII (#sc-391239A) and tamoxifen (#H7904) were from

124 Sigma-Aldrich Co (82024 Taufkirchen, Germany). TRV120055 (#JT-71995) and TRV120056

125 (#JT-71996) were from Synpeptide Co., Ltd (Shanghai, China).

126 **2.3 Mesenteric and cerebral arteries**

127 After mice were killed, the mesenteric bed and brain were removed and placed into cold (4°C),

128 gassed (95% O_2-5% CO_2) physiological saline solution (PSS) of the following composition

129 (mmol/L): 119 NaCl, 4.7 KCl, 25 $NaHCO_3$, 1.2 KH_2PO_4, 1.6 $CaCl_2$, 1.2 $MgSO_4$, 0.03 EDTA,

130   and 11.1 glucose. Third or fourth order mesenteric and middle cerebral arteries or posterior

131   cerebral arteries were dissected and cleaned of adventitial connective tissue (46) (18) (10)

132   (11).

133   **2.4 Pressure myography**

134   Vessel myography was performed as previously described (26) (37) (46) (10). Mesenteric or

135   cerebral arteries were mounted on glass cannula and superfused continuously with PSS (95%

136   O_2-5% CO_2; pH, 7.4; 37°C). The vessels were stepwise pressurized to 20, 40, 60, 80, or 100

137   mmHg using a pressure servo control system (Living System Instrumentation, Burlington, VT).

138   We measured the inner diameter of the vessels with a video microscope (Nikon Diaphot,

139   Düsseldorf, Germany) connected to a personal computer for data acquisition and analysis

140   (HaSoTec, Rostock, Germany) (18) (19) (46) (11) (10). Arteries were equilibrated for 45 to 60

141   minutes before starting experiments. A 60-mmol/L KCl challenge was performed before any

142   other intervention.

143   **2.5 Analysis of myogenic tone in isolated perfused kidneys**

144   Isolated kidneys were perfused in an organ chamber using a peristaltic pump at constant flow

145   (0.3-1.9 ml/min) of oxygenated (95% O_2 and 5% CO_2) PSS (46). Drugs (Ang II or biased

146   agonists) were added to the perfusate. Perfusion pressure was measured by a pressure

147   transducer after an equilibration period of 60-90 min. Data were recorded and analyzed by a

148   Powerlab acquisition system (AD Instruments, Colorado Springs). Ang II-induced pressor

149   effects were normalized to the maximal pressor effect induced by KCl (60 mmol/L) (37) (46)

150   (18).

151   **2.6 Immunofluorescence**

152   *Agtr1a$^{+/+}$* and SM-*Agtr1a$^{-/-}$* mice mesenteric arteries were dissected and further fixed in 4%

153   formaldehyde and embedded in Tissue-Tek O.C.T. compound to be frozen in liquid nitrogen.

154   Tissues were then sectioned and permeabilized in 1% Triton X-100 in PBS. Sections were

155   stained with the primary antibody overnight at 4°C. After washing with PBS for 3×5 min, the

156   secondary antibody and DAPI were applied for 2 hours at room temperature. Fluorescence

157   images were captured by use of Olympus FV1000 confocal microscopy and images were

158   analyzed by ImageJ analysis software.

159   **2.7 Statistics**

160   Data are presented as means ± SEM. Statistically significant differences in mean values were

161   determined by Student's unpaired t test or one-way analysis of variance (ANOVA). P values <

162   0.05 were considered statistically significant.

163

3. Results

3.1 AT1aR is essential for pressure-induced response in the renal circulation

We evaluated myogenic tone in mouse renal circulation, a highly myogenic bed regulating blood flow to the kidneys and consequently sodium excretion and systemic blood pressure. Renal vascular resistance of isolated perfused kidneys was determined by measuring perfusion pressure at fixed levels of flow. The perfusion pressure increased with flow rate in kidneys of wild-type $Agtr1a^{+/+}$ mice, reaching a value of about 160 mmHg at a flow rate of 1.9 ml/min (**Figure 2A**). Kidneys from $Agtr1a^{-/-}$ mice developed significantly less pressure at the same flow rate (**Figure 2B, E**). 60 mmol/L KCl-induced increases in perfusion pressure were normal in $Agtr1a^{-/-}$ kidneys (**Figure 2 F**). At a flow rate of 1.9 ml/min, pressure in $Agtr1a^{-/-}$ kidneys was ~100 mmHg lower than in $Agtr1a^{+/+}$ kidneys. Angiotensin II (Ang II, 10 nmol/L) increased perfusion pressure by ~80 mmHg in kidneys of $Agtr1a^{+/+}$ mice, but had no effect in kidneys of $Agtr1a^{-/-}$ mice (**Figure 2C**); this is indicative of AT1aRs mediating Ang II-dependent vasoconstriction. Removal of external Ca^{2+} nearly abolished flow-induced myogenic constriction in perfused kidneys of $Agtr1a^{+/+}$ mice, but had nearly no effect in kidneys of $Agtr1a^{-/-}$ mice (**Figure 2D**), indicating AT1aRs mediate also myogenic constriction of mouse renal arterioles. Of note, there was no difference in myogenic tone and Ang II vasoconstrictions between $Agtr1b^{-/-}$ versus $Agtr1b^{+/+}$ kidneys (**Figure 3**).

Next we focused on kidneys from SM-$Agtr1a^{-/-}$ mice (**Figure 4**). At a flow rate of 1.9 ml/min, pressure in SM-$Agtr1a^{-/-}$ kidneys was ~90 mmHg lower than in $Agtr1a^{+/+}$ kidneys (**Figure 4 A, B, E**). SM-$Agtr1a^{-/-}$ kidneys showed largely reduced myogenic vasoconstriction as assessed by exposure of the kidneys to Ca^{2+} free PSS (**Figure 4B**, **D**), whereas wild-type kidneys showed strong myogenic vasoconstrictions (**Figure 4A, D**). 60 mmol/L KCl-induced increases in perfusion pressure were normal in $Agtr1a^{-/-}$ kidneys (**Figure 4F**). Ang II (10 nmol/L) induced weaker increases in perfusion pressure in kidneys of SM-$Agtr1a^{-/-}$ mice compared to controls (**Figure 4D**). Together, these results reveal a key role of AT1aR but not AT1bR in the flow-induced myogenic response of the mouse renal vasculature.

3.2 AT1aR contribute to myogenic constriction in mesenteric arteries

We monitored myogenic constriction in resistance-sized mesenteric arteries using videomicroscopy. Mesenteric arteries were exposed to stepwise (20 mmHg) increases in intraluminal pressure (20-100 mmHg) in the presence and absence of external Ca^{2+} (1.6 mmol/L) to determine active and passive vessel diameters, respectively. **Figure 5** shows

196   representative recordings of mesenteric arteries from $Agtr1a^{+/+}$ mice (**Figure 5A**) and

197   SM-$Agtr1a^{-/-}$ mice (**Figure 5B**) and myogenic vasoconstriction was defined as the diameter

198   difference in the presence and absence of external Ca^{2+} (1.6 mmol/L) at each pressure step

199   (46). Increases in intraluminal pressure generated active tension that counteracted further

200   dilation of the vessels at 60 to 80 mmHg in mesenteric arteries from $Agtr1a^{+/+}$ mice, reaching

201   peak constrictions of 50 μm at 80 to 100 mmHg (**Figure 5A**). In contrast, mesenteric arteries

202   from SM-$Agtr1a^{-/-}$ mice only produced ~35% of the constriction observed in wild-type arteries

203   (**Figure 5B, C**). Ang II strongly constricted arteries from $Agtr1a^{+/+}$ mice but had no effect on

204   arteries from SM-$Agtr1a^{-/-}$ mice (**Figure 5D**); the latter did constrict in response to 60 mmol/L

205   KCl (**Figure 5E**). This study observed a marked reduction in AT1aR expression in the media

206   of SM-$Agtr1a^{-/-}$ mesenteric arteries compared to wild-type (**Figure 1B**), in keeping with this

207   receptor mediating myogenic constriction in mesenteric arteries.

208   **3.3 AT1aR contribute to myogenic constriction in cerebral arteries**

209   Next, we studied the function of AT1aRs in cerebral arteries. Vessels were equilibrated at 15

210   mmHg (30 min) and following an assessment of KCl-induced constriction, arteries were

211   pressurized to 80 mmHg (**Figure 6A**). Ang II constrictions and myogenic constriction was

212   significantly decreased in SM-$Agtr1a^{-/-}$ arteries compared to wild-type (**Figure 6A, B, C, D**).

213   Both wild-type and SM-$Agtr1a^{-/-}$ arteries produced similar constrictions when exposed to 60

214   mmol/L KCl (**Figure 6E**). The results demonstrate a key role of AT1aR in the myogenic

215   response of mouse cerebral arteries.

216   **3.4 $G_{q/11}$ protein dependent signaling pathway is responsible for myogenic tone**

217   To explore the role of $G_{q/11}$ and β-arrestin signaling pathways downstream of AT1R, we used

218   the biased agonists TRV120055 and SII to activate $G_{q/11}$ and β-arrestin signaling pathways,

219   respectively (29) (34) (51). We found that TRV120055 increased vascular tone in mesenteric

220   arteries (**Figure 7A, B)**, whereas SII had no effect (**Figure 7C, D**). Similarly, TRV120055 and

221   TRV120056 (another biased $G_{q/11}$ coupled AT1R agonist) enhanced dose-dependent

222   perfusion pressure in isolated kidneys (**Figure 8A, C**), whereas SII had no effect (**Figure 8B,**

223   **C**). The removal of external Ca^{2+} abolished agonist-induced vasoconstrictions in perfused

224   kidneys (**Figure 8D**), indicating AT1aRs mediate vasoconstriction *via* canonical $G_{q/11}$ but not

225   noncanonical β-arrestin pathways. To confirm the results, we next examined the effects of

226   FR900359, a selective $G_{q/11}$-protein inhibitor (23) (47) (35). FR900359 abolished both

227   myogenic and Ang II-dependent constrictions in renal arterioles (**Figure 9**) and mesenteric

228   arteries (**Figure 7E, F**). These results indicate that myogenic vasoconstriction is mediated

229   through the mechanosensitive AT1aR and the canonical $G_{q/11}$ signaling pathway.

4. Discussion

231   The study found that the canonical $G_{q/11}$ signaling of mechanoactivated AT1aR is responsible

232   for myogenic vasoconstriction in mesenteric, renal arteries and cerebral arteries. We

233   observed a loss of myogenic autoregulation in the renal circulation of $Agtr1a^{-/-}$ mice, an effect

234   which was normal in $Agtr1b^{-/-}$ mice. Similarly, we found that myogenic tone was strongly

235   reduced in two other myogenic arteries (mesentery and cerebral) from smooth muscle

236   specific AT1aR-deficient (SM-$Agtr1a^{-/-}$) mice compared to wild-type. Using the

237   pharmacological $G_{q/11}$ inhibitor FR900359 and several GPCR biased agonists, we showed

238   that AT1Rs cause vasoconstriction *via* canonical $G_{q/11}$ signaling but not alternative G protein

239   signaling downstream of the AT1R.

240   *AT1aRs are primary mechanosensors in intact arteries*

241   Multiple GPCRs have been proposed to act as mechanosensors to regulate myogenic tone in

242   resistance arteries. While stretch induces activation of purinergic P2Y6 UDP receptors,

243   thromboxane A2 (TP) receptors and sphingosine-1-phosphate (S1P) receptors in certain

244   vascular beds (27) (28) (30), the AT1R remains one of the best characterized mechanosensor

245   in the vasculature (49) (55). Humans express a single type of AT1R, whereas two isoforms

246   (AT1aR and AT1bR) are present in rodents (36) (53). Using $Agtr1a^{-/-}$ mice and inverse AT1R

247   agonist, our previous data suggested that ligand-independent AT1aR activation is required for

248   myogenic response in resistance mesenteric arteries and renal arterioles (46). However, two

249   recent studies reported that myogenic tone was diminished in $Agtr1b^{-/-}$ mesenteric and

250   cerebral arteries, which implies a possible role of AT1bRs in mechanosensation (42) (3). In

251   contrast, we found that myogenic tone was normal in $Agtr1b^{-/-}$ perfused kidneys, which argues

252   against a role of AT1bR in myogenic constriction in the renal circulation. This data was,

253   however, obtained in global mutant mice, which often display compensatory mechanisms for

254   the lack of AT1Rs. Moreover, AT1aR and AT1bR are expressed at similar levels in cerebral

255   parenchymal arterioles and genetic knockout of AT1aR (but not AT1bR) blunted the ability of

256   these vessels to generate myogenic tone (52). The latter effect is opposite to cerebral arteries

257   where genetic knockout of AT1bR blunted the ability to develop myogenic tone (42). To

258   overcome these potential limitations, we generated tamoxifen-inducible SM-$Agtr1a$

259   (SMMHC-Cre+$Agtr1a^{flox/flox}$) mice for careful phenotypic investigation. We found that myogenic

260   constriction was impaired in cerebral, mesenteric and renal arteries isolated from smooth

261   muscle AT1aR-deficient mice. The data provide firm evidence that AT1aRs play a key role as

262   mechanosensors mediating myogenic constriction in the murine vasculature.

263   *AT1aRs downstream signaling to cause vasoconstriction*

264   We next explored downstream signaling pathways mediated by $G_{q/11}$ and/or β arrestins of the

265   AT1R in the vascular response. In cell culture, osmotic cell stretch has been found to increase

266   the binding affinity and potency of the β-arrestin-biased agonist TRV120023 with no effect on

267   the balanced agonist Ang II through AT1R to induce a conformation change of β-arrestin 2,

268   similar to that induced by β-arrestin-biased agonists (50). Similarly, hypo-osmotic stretch

269   induced β-arrestin-biased signaling of AT1Rs in the absence of G protein activation (44). We

270   failed to observe β-arrestin mediated enhancement of myogenic vasoconstriction with the

271   β-arrestin biased agonist SII in intact arteries (mesenteric and renal arteries: **Figure 10**). The

272   discrepancy might be caused by differences between the hypo-osmotic cell swelling and

273   tensile stretch on the smooth muscle cell layer in intact arteries to cause mechanoactivation of

274   AT1aRs *in situ*. GPCRs biased mechanisms have been described between two different G

275   proteins, between β-arrestin-1 and 2, and between different states of the same receptor

276   bound to different ligands (12) (21) (54). However, the majority of well described GPCRs

277   biased ligand examples refers to selective G protein signaling versus β-arrestin-mediated

278   signaling (20) (33) (43) (51). AT1aR is one of the best characterized GPCR enabling biased

279   receptor signaling. It can be activated in either a canonical G protein-dependent signaling

280   mode (5) (37) or noncanonical β-arrestin-mediated signaling mode (44) (50). In line, we found

281   that the natural biased agonist Ang II was able to increase G protein signaling of

282   mechanoactivated AT1R receptors to enhance the vasoconstrictor response.

283   We hypothesized that $G_{q/11}$ signaling contributes to myogenic tone in mesenteric and

284   renal arteries and consistent with this idea, we found that the vasoconstrictor responses were

285   strongly increased by the $G_{q/11}$ AT1R biased agonists TRV120055 and TRV20056 (**Figure 10**).

286   Moreover, we found that the $G_{q/11}$ blocker FR900359 inhibited both myogenic tone and Ang II

287   induced constrictions in mesenteric arteries and renal arterioles (**Figure 10**). The data imply

288   that myogenic vasoconstriction requires canonical $G_{q/11}$ signaling of the AT1aR. Consistently,

289   myogenic tone is increased in the absence of regulator of G-protein signaling 2 (RGS2),

290   which is an endogenous terminator of Galpha$_{q/11}$ (G$\alpha_{q/11}$) signaling (19) (37). The data align

291   with findings indicating that mechanically activated AT1R generate diacylglycerol, which in

292   turn activates protein kinase C (PKC) and induces the actin cytoskeleton reorganization

293   necessary for pressure-induced vasoconstriction (22). Finally, our conclusions are supported

294   by findings indicating that another $G_{q/11}$-protein inhibitor YM 254890 profoundly reduced

295 myogenic tone in mesenteric arteries (49). Note, this data contrast with recent findings, which

296 proposed that $G_{12/13}$- and Rho/Rho kinase-mediated signaling is required in myogenic

297 vasoconstriction by inhibition of myosin phosphatase (5). The reason for the discrepancy is

298 presently unknown, but may depend on which vessel order was utilized, i.e. 3rd or 4th order

299 mesenteric versus 1st or 2nd order mesenteric arteries. Moreover, the myogenic response was

300 only reduced by 50% in $G_{12/13}$-deficient cerebral arteries (5), which may indicate that this

301 pathway may play a role in some but not all vessels. Thus, it is possible that the relevance to

302 the two signaling pathway differs between various vascular beds and artery branches. Our

303 study provides firm evidence that AT1aRs coupled to $G_{q/11}$ signaling is an essential

304 component of dynamic mechanochemical signaling in arterial vascular smooth muscle cells

305 causing myogenic tone (**Figure 10**).

306   Signaling of most GPCRs *via* G proteins is terminated (desensitization) by the

307 phosphorylation of active receptor by specific kinases (GPCR kinases, or GRKs) and

308 subsequent binding of ß-arrestins that selectively recognize active phosphorylated receptors.

309 Although, GRKs and ß-arrestins play also a role in multiple noncanonical signaling pathways

310 in the cell, both GPCR-initiated and receptor-independent (32) (15), our study failed to

311 demonstrate that this pathway plays an important role in the myogenic response (**Figure 10**).

312 Thus, it is unlikely that blood pressure lowering effects of ß-arrestin biased AT1R agonists,

313 e.g. Trevena 120027 (4), are caused by direct effects of this GPCR in the arterial smooth

314 muscle cells.

315   In summary, we provide new and firm evidence for a mechanosensitive function of

316 AT1aR in myogenic vasoconstriction in mesenteric, renal and cerebral arteries, i.e. in three

317 different highly myogenic vascular beds. Our study clearly shows that mechanical stress

318 activates AT1R in arterial smooth muscle cells, which subsequently triggers canonical $G_{q/11}$

319 signaling, irrespective of GRK/β-arrestin signaling, to cause myogenic vasoconstriction. Our

320 results argue against the idea of multiple mechanosensors coupled to noncanonical β-arrestin

321 pathways generating myogenic arterial tone. These findings lay ground for additional studies

322 to characterize the molecular mechanisms of mechanoactivated AT1aR coupled to $G_{q/11}$

323 signaling in intact arteries, which may reveal new molecular targets for drug development to

324 alleviate increased or dysregulated arterial tone in hypertension and other cardiovascular

325 diseases.

326

327 **Acknowledgments**

331

332 **References**

333 1. **Balakumar P and Jagadeesh G.** A century old renin-angiotensin system still grows

334 with endless possibilities: AT1 receptor signaling cascades in cardiovascular

335 physiopathology. *Cell Signal* 26: 2147-2160, 2014.

336 2. **Bayliss WM.** On the local reactions of the arterial wall to changes of internal

337 pressure. *The Journal of physiology* 28: 220-231, 1902.

338 3. **Blodow S, Schneider H, Storch U, Wizemann R, Forst AL, Gudermann T, and**

339 **Mederos y Schnitzler M.** Novel role of mechanosensitive AT1B receptors in myogenic

340 vasoconstriction. *Pflugers Archiv : European journal of physiology* 466: 1343-1353, 2014.

341 4. **Boerrigter G, Lark MW, Whalen EJ, Soergel DG, Violin JD, and Burnett JC, Jr.**

342 Cardiorenal actions of TRV120027, a novel ss-arrestin-biased ligand at the angiotensin II

343 type I receptor, in healthy and heart failure canines: a novel therapeutic strategy for

344 acute heart failure. *Circ Heart Fail* 4: 770-778, 2011.

345 5. **Chennupati R, Wirth A, Favre J, Li R, Bonnavion R, Jin Y-J, Wietelmann A,**

346 **Schweda F, Wettschureck N, Henrion D, and Offermanns S.** Myogenic

347 vasoconstriction requires G/G and LARG to maintain local and systemic vascular

348 resistance. *Elife* 8, 2019.

349 6. **Cipolla MJ and Curry AB.** Middle cerebral artery function after stroke: the

350 threshold duration of reperfusion for myogenic activity. *Stroke* 33: 2094-2099, 2002.

351 7. **Coats P, Johnston F, MacDonald J, McMurray JJ, and Hillier C.** Signalling

352 mechanisms underlying the myogenic response in human subcutaneous resistance

353 arteries. *Cardiovascular research* 49: 828-837, 2001.

354 8. **Davis MJ.** Perspective: physiological role(s) of the vascular myogenic response.

355 *Microcirculation (New York, NY : 1994)* 19: 99-114, 2012.

356 9. **Davis MJ and Hill MA.** Signaling mechanisms underlying the vascular myogenic

357 response. *Physiol Rev* 79: 387-423, 1999.

358 10. **Ercu M, Marko L, Schachterle C, Tsvetkov D, Cui Y, Maghsodi S, Bartolomaeus**

359 **TUP, Maass PG, Zuhlke K, Gregersen N, Hubner N, Hodge R, Muhl A, Pohl B,**

360 **Mole-Illas R, Geelhaar A, Walter S, Napieczynska H, Schelenz S, Taube M, Heuser A,**

361 **Anistan YM, Qadri F, Todiras M, Plehm R, Popova E, Langanki R, Eichhorst J,**
362 **Lehmann M, Wiesner B, Russwurm M, Forslund SK, Kamer I, Muller DN, Gollasch M,**
363 **Aydin A, Bahring S, Bader M, Luft FC, and Klussmann E.** Phosphodiesterase 3A and
364 Arterial Hypertension. *Circulation*, 2020.

365 11. **Fan G, Kassmann M, Cui Y, Matthaeus C, Kunz S, Zhong C, Zhu S, Xie Y, Tsvetkov**
366 **D, Daumke O, Huang Y, and Gollasch M.** Age attenuates the T-type CaV 3.2-RyR axis in
367 vascular smooth muscle. *Aging Cell* 19: e13134, 2020.

368 12. **Gesty-Palmer D, Chen M, Reiter E, Ahn S, Nelson CD, Wang S, Eckhardt AE,**
369 **Cowan CL, Spurney RF, Luttrell LM, and Lefkowitz RJ.** Distinct beta-arrestin- and G
370 protein-dependent pathways for parathyroid hormone receptor-stimulated ERK1/2
371 activation. *The Journal of biological chemistry* 281: 10856-10864, 2006.

372 13. **Groneberg D, Konig P, Wirth A, Offermanns S, Koesling D, and Friebe A.** Smooth
373 muscle-specific deletion of nitric oxide-sensitive guanylyl cyclase is sufficient to induce
374 hypertension in mice. *Circulation* 121: 401-409, 2010.

375 14. **Gschwend S, Henning RH, Pinto YM, de Zeeuw D, van Gilst WH, and Buikema H.**
376 Myogenic constriction is increased in mesenteric resistance arteries from rats with
377 chronic heart failure: instantaneous counteraction by acute AT1 receptor blockade.
378 *British journal of pharmacology* 139: 1317-1325, 2003.

379 15. **Gurevich VV and Gurevich EV.** GPCR Signaling Regulation: The Role of GRKs and
380 Arrestins. *Front Pharmacol* 10: 125, 2019.

381 16. **Hansen PB, Jensen BL, Andreasen D, and Skøtt O.** Differential expression of T-
382 and L-type voltage-dependent calcium channels in renal resistance vessels. *Circulation*
383 *research* 89: 630-638, 2001.

384 17. **Harder DR.** Pressure-dependent membrane depolarization in cat middle cerebral
385 artery. *Circulation research* 55: 197-202, 1984.

386 18. **Heinze C, Seniuk A, Sokolov MV, Huebner AK, Klementowicz AE, Szijarto IA,**
387 **Schleifenbaum J, Vitzthum H, Gollasch M, Ehmke H, Schroeder BC, and Hubner CA.**
388 Disruption of vascular Ca2+-activated chloride currents lowers blood pressure. *J Clin*
389 *Invest* 124: 675-686, 2014.

390 19. **Hercule HC, Tank J, Plehm R, Wellner M, da Costa Goncalves AC, Gollasch M,**
391 **Diedrich A, Jordan J, Luft FC, and Gross V.** Regulator of G protein signalling 2
392 ameliorates angiotensin II-induced hypertension in mice. *Exp Physiol* 92: 1014-1022,
393 2007.

394   20. **Hodavance SY, Gareri C, Torok RD, and Rockman HA.** G Protein–coupled Receptor
395   Biased Agonism. *Journal of Cardiovascular Pharmacology* 67: 193-202, 2016.

396   21. **Hoffmann C, Ziegler N, Reiner S, Krasel C, and Lohse MJ.** Agonist-selective,
397   receptor-specific interaction of human P2Y receptors with beta-arrestin-1 and -2. *The*
398   *Journal of biological chemistry* 283: 30933-30941, 2008.

399   22. **Hong K, Zhao G, Hong Z, Sun Z, Yang Y, Clifford PS, Davis MJ, Meininger GA, and**
400   **Hill MA.** Mechanical activation of angiotensin II type 1 receptors causes actin
401   remodelling and myogenic responsiveness in skeletal muscle arterioles. *J Physiol* 594:
402   7027-7047, 2016.

403   23. **Inamdar V, Patel A, Manne BK, Dangelmaier C, and Kunapuli SP.**
404   Characterization of UBO-QIC as a Galphaq inhibitor in platelets. *Platelets* 26: 771-778,
405   2015.

406   24. **Ito M, Oliverio MI, Mannon PJ, Best CF, Maeda N, Smithies O, and Coffman TM.**
407   Regulation of blood pressure by the type 1A angiotensin II receptor gene. *Proc Natl Acad*
408   *Sci U S A* 92: 3521-3525, 1995.

409   25. **Jarve A, Todiras M, Lian X, Filippelli-Silva R, Qadri F, Martin RP, Gollasch M, and**
410   **Bader M.** Distinct roles of angiotensin receptors in autonomic dysreflexia following
411   high-level spinal cord injury in mice. *Exp Neurol* 311: 173-181, 2019.

412   26. **Kaßmann M, Szijártó IA, García-Prieto CF, Fan G, Schleifenbaum J, Anistan Y-M,**
413   **Tabeling C, Shi Y, le Noble F, Witzenrath M, Huang Y, Markó L, Nelson MT, and**
414   **Gollasch M.** Role of Ryanodine Type 2 Receptors in Elementary Ca Signaling in Arteries
415   and Vascular Adaptive Responses. *J Am Heart Assoc* 8: e010090, 2019.

416   27. **Kauffenstein G, Laher I, Matrougui K, Guérineau NC, and Henrion D.** Emerging
417   role of G protein-coupled receptors in microvascular myogenic tone. *Cardiovascular*
418   *research* 95: 223-232, 2012.

419   28. **Kauffenstein G, Tamareille S, Prunier F, Roy C, Ayer A, Toutain B, Billaud M,**
420   **Isakson BE, Grimaud L, Loufrani L, Rousseau P, Abraham P, Procaccio V, Monyer H,**
421   **de Wit C, Boeynaems J-M, Robaye B, Kwak BR, and Henrion D.** Central Role of P2Y6
422   UDP Receptor in Arteriolar Myogenic Tone. *Arteriosclerosis, thrombosis, and vascular*
423   *biology* 36: 1598-1606, 2016.

424   29. **Kendall RT, Strungs EG, Rachidi SM, Lee M-H, El-Shewy HM, Luttrell DK, Janech**
425   **MG, and Luttrell LM.** The beta-arrestin pathway-selective type 1A angiotensin receptor
426   (AT1A) agonist [Sar1,Ile4,Ile8]angiotensin II regulates a robust G protein-independent

427   signaling network. *The Journal of biological chemistry* 286: 19880-19891, 2011.

428   30. **Kroetsch JT and Bolz S-S.** The TNF-α/sphingosine-1-phosphate signaling axis

429   drives myogenic responsiveness in heart failure. *Journal of vascular research* 50: 177-185,

430   2013.

431   31. **Ledoux J, Gee DM, and Leblanc N.** Increased peripheral resistance in heart failure:

432   new evidence suggests an alteration in vascular smooth muscle function. *British journal*

433   *of pharmacology* 139: 1245-1248, 2003.

434   32. **Lefkowitz RJ.** A brief history of G-protein coupled receptors (Nobel Lecture). *Angew*

435   *Chem Int Ed Engl* 52: 6366-6378, 2013.

436   33. **Lefkowitz RJ.** Historical review: a brief history and personal retrospective of

437   seven-transmembrane receptors. *Trends in pharmacological sciences* 25: 413-422, 2004.

438   34. **Li W, Xu J, Kou X, Zhao R, Zhou W, and Fang X.** Single-molecule force spectroscopy

439   study of interactions between angiotensin II type 1 receptor and different biased ligands

440   in living cells. *Anal Bioanal Chem* 410: 3275-3284, 2018.

441   35. **Lian X, Beer-Hammer S, Konig GM, Kostenis E, Nurnberg B, and Gollasch M.**

442   RXFP1 Receptor Activation by Relaxin-2 Induces Vascular Relaxation in Mice via a

443   Galphai2-Protein/PI3Kss/gamma/Nitric Oxide-Coupled Pathway. *Front Physiol* 9: 1234,

444   2018.

445   36. **Madhun ZT, Ernsberger P, Ke FC, Zhou J, Hopfer U, and Douglas JG.** Signal

446   transduction mediated by angiotensin II receptor subtypes expressed in rat renal

447   mesangial cells. *Regul Pept* 44: 149-157, 1993.

448   37. **Mederos y Schnitzler M, Storch U, Meibers S, Nurwakagari P, Breit A, Essin K,**

449   **Gollasch M, and Gudermann T.** Gq-coupled receptors as mechanosensors mediating

450   myogenic vasoconstriction. *Embo j* 27: 3092-3103, 2008.

451   38. **Moosmang S, Schulla V, Welling A, Feil R, Feil S, Wegener JW, Hofmann F, and**

452   **Klugbauer N.** Dominant role of smooth muscle L-type calcium channel Cav1.2 for blood

453   pressure regulation. *Embo j* 22: 6027-6034, 2003.

454   39. **Nelson MT, Patlak JB, Worley JF, and Standen NB.** Calcium channels, potassium

455   channels, and voltage dependence of arterial smooth muscle tone. *Am J Physiol* 259:

456   C3-18, 1990.

457   40. **Oliverio MI, Kim HS, Ito M, Le T, Audoly L, Best CF, Hiller S, Kluckman K, Maeda**

458   **N, Smithies O, and Coffman TM.** Reduced growth, abnormal kidney structure, and type

459   2 (AT2) angiotensin receptor-mediated blood pressure regulation in mice lacking both

AT1A and AT1B receptors for angiotensin II. *Proceedings of the National Academy of Sciences of the United States of America* 95: 15496-15501, 1998.

41. **Pires PW, Jackson WF, and Dorrance AM.** Regulation of myogenic tone and structure of parenchymal arterioles by hypertension and the mineralocorticoid receptor. *Am J Physiol Heart Circ Physiol* 309: H127-136, 2015.

42. **Pires PW, Ko EA, Pritchard HAT, Rudokas M, Yamasaki E, and Earley S.** The angiotensin II receptor type 1b is the primary sensor of intraluminal pressure in cerebral artery smooth muscle cells. *J Physiol (Lond)* 595: 4735-4753, 2017.

43. **Rajagopal S, Ahn S, Rominger DH, Gowen-MacDonald W, Lam CM, Dewire SM, Violin JD, and Lefkowitz RJ.** Quantifying ligand bias at seven-transmembrane receptors. *Mol Pharmacol* 80: 367-377, 2011.

44. **Rakesh K, Yoo B, Kim IM, Salazar N, Kim KS, and Rockman HA.** beta-Arrestin-biased agonism of the angiotensin receptor induced by mechanical stress. *Sci Signal* 3: ra46, 2010.

45. **Sauvé M, Hui SK, Dinh DD, Foltz WD, Momen A, Nedospasov SA, Offermanns S, Husain M, Kroetsch JT, Lidington D, and Bolz S-S.** Tumor Necrosis Factor/Sphingosine-1-Phosphate Signaling Augments Resistance Artery Myogenic Tone in Diabetes. *Diabetes* 65: 1916-1928, 2016.

46. **Schleifenbaum J, Kassmann M, Szijarto IA, Hercule HC, Tano JY, Weinert S, Heidenreich M, Pathan AR, Anistan YM, Alenina N, Rusch NJ, Bader M, Jentsch TJ, and Gollasch M.** Stretch-activation of angiotensin II type 1a receptors contributes to the myogenic response of mouse mesenteric and renal arteries. *Circ Res* 115: 263-272, 2014.

47. **Schrage R, Schmitz A-L, Gaffal E, Annala S, Kehraus S, Wenzel D, Büllesbach KM, Bald T, Inoue A, Shinjo Y, Galandrin S, Shridhar N, Hesse M, Grundmann M, Merten N, Charpentier TH, Martz M, Butcher AJ, Slodczyk T, Armando S, Effern M, Namkung Y, Jenkins L, Horn V, Stößel A, Dargatz H, Tietze D, Imhof D, Galés C, Drewke C, Müller CE, Hölzel M, Milligan G, Tobin AB, Gomeza J, Dohlman HG, Sondek J, Harden TK, Bouvier M, Laporte SA, Aoki J, Fleischmann BK, Mohr K, König GM, Tüting T, and Kostenis E.** The experimental power of FR900359 to study Gq-regulated biological processes. *Nature Communications* 6, 2015.

48. **Sparks MA, Parsons KK, Stegbauer J, Gurley SB, Vivekanandan-Giri A, Fortner CN, Snouwaert J, Raasch EW, Griffiths RC, Haystead TAJ, Le TH, Pennathur S, Koller B, and Coffman TM.** Angiotensin II type 1A receptors in vascular smooth muscle cells do

493   not influence aortic remodeling in hypertension. *Hypertension (Dallas, Tex : 1979)* 57:
494   577-585, 2011.

495   49. **Storch U, Blodow S, Gudermann T, and Mederos Y Schnitzler M.** Cysteinyl
496   leukotriene 1 receptors as novel mechanosensors mediating myogenic tone together
497   with angiotensin II type 1 receptors-brief report. *Arteriosclerosis, thrombosis, and*
498   *vascular biology* 35: 121-126, 2015.

499   50. **Tang W, Strachan RT, Lefkowitz RJ, and Rockman HA.** Allosteric Modulation of
500   β-Arrestin-biased Angiotensin II Type 1 Receptor Signaling by Membrane Stretch.
501   *Journal of Biological Chemistry* 289: 28271-28283, 2014.

502   51. **Wei H, Ahn S, Shenoy SK, Karnik SS, Hunyady L, Luttrell LM, and Lefkowitz RJ.**
503   Independent beta-arrestin 2 and G protein-mediated pathways for angiotensin II
504   activation of extracellular signal-regulated kinases 1 and 2. *Proceedings of the National*
505   *Academy of Sciences of the United States of America* 100: 10782-10787, 2003.

506   52. **Yamasaki E, Thakore P, Krishnan V, and Earley S.** Differential expression of
507   angiotensin II type 1 receptor subtypes within the cerebral microvasculature. *Am J*
508   *Physiol Heart Circ Physiol* 318: H461-H469, 2020.

509   53. **Zhou J, Ernsberger P, and Douglas JG.** A novel angiotensin receptor subtype in rat
510   mesangium. Coupling to adenylyl cyclase. *Hypertension (Dallas, Tex : 1979)* 21:
511   1035-1038, 1993.

512   54. **Zidar DA, Violin JD, Whalen EJ, and Lefkowitz RJ.** Selective engagement of G
513   protein coupled receptor kinases (GRKs) encodes distinct functions of biased ligands.
514   *Proceedings of the National Academy of Sciences of the United States of America* 106:
515   9649-9654, 2009.

516   55. **Zou Y, Akazawa H, Qin Y, Sano M, Takano H, Minamino T, Makita N, Iwanaga K,**
517   **Zhu W, Kudoh S, Toko H, Tamura K, Kihara M, Nagai T, Fukamizu A, Umemura S, Iiri**
518   **T, Fujita T, and Komuro I.** Mechanical stress activates angiotensin II type 1 receptor
519   without the involvement of angiotensin II. *Nat Cell Biol* 6: 499-506, 2004.

520

521   **Figure legends**

522   **Figure 1: Conditional deletion of AT1a receptors in vascular smooth muscle cells of**
523   **arteries. A**: Schematic representation of the mouse allele containing loxP sequences, and the
524   floxed allele after the action of Cre recombinase. **B:** Immunofluorescence staining results
525   show that AT1R (red) is highly expressed in the mesenteric artery of *Agtr1a*^{+/+} mice. In

526   SM-$Agtr1a^{-/-}$ mouse mesenteric artery, the expression of AT1R is specifically reduced in

527   smooth muscle cells. Scale bar: 40 μm.

528   **Figure 2: Vasoregulation in isolated perfused kidneys of $Agtr1a^{-/-}$ mice.   A, B**: Original

529   recordings of perfusion pressure in kidneys of $Agtr1a^{+/+}$ (**A**) and $Agtr1a^{-/-}$ mice (**B**). **C:** Increase

530   in the perfusion pressure induced by 100 nM Ang II. **D:** Myogenic tone assessed by exposure

531   to Ca^{2+} free PSS. **E**: Perfusion pressure at flow rates of 0.3 ml/min, 0.7 ml/min, 1.3 ml/min and

532   1.9 ml/min. **F**: Increase in the perfusion pressure induced by 60mM KCl. n=6 $Agtr1a^{+/+}$ kidneys

533   and n=7 $Agtr1a^{-/-}$ kidneys for all panels. *$p<0.05$; n.s., not significant.

534   **Figure 3: Vasoregulation in isolated perfused kidneys of $Agtr1b^{-/-}$ mice.   A, B**: Original

535   recordings of the perfusion pressure in kidneys of $Agtr1b^{+/+}$ (**A**) and $Agtr1b^{-/-}$ mice (**B**). **C:**

536   Increase in perfusion pressure induced by 10 nM Ang II. **D:** Change of pressure assessed by

537   exposure to Ca^{2+} free PSS. **E**: Perfusion pressure at flow rates of 0.3 ml/min, 0.7 ml/min, 1.3

538   ml/min and 1.9 ml/min. **F**: Increase in perfusion pressure induced by 60 mM KCl. n=6

539    $Agtr1b^{+/+}$ kidneys and n=6 $Agtr1b^{-/-}$ kidneys for all panels. w.o., wash-out; n.s., not significant.

540   **Figure 4: Vasoregulation in isolated perfused kidneys of SM-$Agtr1a^{-/-}$ mice.   A, B**:

541   Original recordings of the perfusion pressure in kidneys of $Agtr1a^{+/+}$ (**A**) and SM-$Agtr1a^{-/-}$ mice

542   (**B**). **C:** Increase in perfusion pressure induced by 10 nM Ang II. **D:** Change of pressure

543   assessed by exposure to Ca^{2+} free PSS. **E**: Perfusion pressure at flow rates of 0.3 ml/min, 0.7

544   ml/min, 1.3 ml/min, and 1.9 ml/min. **F**: Increase in perfusion pressure induced by 60 mM KCl.

545   n=6 $Agtr1a^{+/+}$ kidneys and n=6 SM-$Agtr1a^{-/-}$ kidneys for all panels. *$p<0.05$; n.s., not

546   significant.

547   **Figure 5: Myogenic tone in mesenteric arteries. A, B**: Representative recordings of MA

548   diameter during a series of pressure steps from 20 to 100 mmHg in 20 mmHg increments in

549   control conditions (+Ca^{2+}) and in Ca^{2+} free solution (-Ca^{2+}). Arteries were isolated from

550    $Agtr1a^{+/+}$ **(A)** and SM-$Agtr1a^{-/-}$ mice **(B)**. Note the increase in active constriction over the entire

551   pressure range from 60 to 100 mmHg in vessels from $Agtr1a^{+/+}$, but not from SM-$Agtr1a^{-/-}$

552   mice. Vasodilation in Ca^{2+}-free solution was observed in $Agtr1a^{+/+}$ but not in SM-$Agtr1a^{-/-}$

553   arteries ($P<0.05$). **C**: Myogenic tone (at 80 mmHg) expressed as dilation of vessels induced

554   by external Ca^{2+} free solution (0 Ca/EGTA; n=6). **D** to **G**: Response to angiotensin II (Ang II;

555   **D, E**) and 60 mM KCl (**F, G**) in MA of $Agtr1a^{+/+}$ and SM-$Agtr1a^{-/-}$ mice. MAs were pressurized

556 to 60 mmHg. Responses are expressed as relative changes in vessel inner diameter.

557 $Agtr1a^{+/+}$, n=5 vessels and SM-$Agtr1a^{-/-}$, n=4 vessels for each group. *p<0.05.

558 **Figure 6: Myogenic tone in cerebral arteries. A, B**: Representative recordings of

559 middle/posterior cerebral arteries diameter at the pressure of 80 mmHg in control conditions

560 (WT), Ang II 100 nmol/L, and in Ca^{2+} free solution. **C**: Myogenic tone (at 80 mmHg) expressed

561 as dilation of vessels induced by external Ca^{2+} free solution. **D, E**: Response to Ang II **(D)** and

562 60 mM KCl **(E)** in middle/posterior cerebral arteries of $Agtr1a^{+/+}$ and SM-$Agtr1a^{-/-}$ mice.

563 $Agtr1a^{+/+}$, n=6 vessels and SM-$Agtr1a^{-/-}$, n=6 vessels for each group. * p<0.05.

564 **Figure 7: Enhancement of the vascular tone by TRV120055. A, C, and E** Representative

565 recordings of mesenteric artery diameter during a series of pressure steps from 20 to 100

566 mmHg in 20 mmHg increments in control conditions (+Ca^{2+}), TRV120055 100 nmol/L **(A)**, SII

567 100 nmol/L **(C)**, FR120055 1 μmol/L **(E)** and in Ca^{2+}-free solution. **B, D and F**: Average

568 myogenic constriction of mesenteric arteries in drug-free physiological salt solution (PSS) and

569 in PSS containing 100 nmol/L TRV120055 **(B)**, 100 nmol/L SII **(D)**, and 1 μmol/L FR120055

570 **(F)** (n=6, 4 and 4, respectively). **G and H:** Response to Ang II in MA in drug-free PSS and

571 PSS in presence of FR120055 at 80 mmHg (n=6 each). *p<0.05; n.s., not significant.

572 **Figure 8: Function of biased AT1R agonists to vasoregulation in isolated perfused**

573 **kidneys from $Agtr1a^{+/+}$ mice.   A, B**: Original recordings of perfusion pressure in response

574 to various flow rates (in ml/min), TRV120055 (**A**) or Sar-Ile II (**B**), Ca^{2+} free perfusion solution

575 (PSS Ca^{2+} free) and re-exposure of the kidneys to PSS. **C:** Increase in perfusion pressure

576 induced by TRV120055 and Sar-Ile II in various concentrations (10 nM to1 μM). **D:** Change of

577 perfusion pressure assessed by exposure of the kidneys to Ca^{2+} free PSS at the presence of

578 TRV120055 or Sar-Ile II at the concentration of 100 nM. **E**: Dose-response relationships for

579 TRV120055 and TRV120056. **F**: Increase in perfusion pressure induced by 60 mM KCl.

580 TRV120055, TRV120056, Sar-Ile II. n=6 kidneys in each group; n=6 kidneys in the control

581 group. *p<0.05; n.s., not significant; Control, $Agtr^{+/+}$ without biased ligand.

582 **Figure 9: Vasoregulation in isolated perfused kidneys of $Agtr1a^{+/+}$ mice pretreated with**

583 **300 nM $G_{q/11}$ blocker FR900359. A**: Original recordings of perfusion pressure in kidneys of

584 $Agtr^{+/+}$ mice in response to various concentrations of Angiotensin II (Ang II) **B**: same as A but

585 pretreated with 300 nM FR900359 for 30 minutes. **C:** Increases in perfusion pressure induced

19

586   by Ang II (1 nM to 1 µM). **D:** Myogenic tone assessed by exposure of the kidneys to Ca^{2+}-free

587   PSS. **E**: Increase in perfusion pressure induced by 60 mM KCl. n=5 *Agtr*$^{+/+}$ kidneys and n=6

588   *Agtr1a*$^{+/+}$ kidneys pretreated with FR900359 for all panels. *p<0.05; w.o., wash-out; n.s., not

589   significant.

590   **Figure 10:** Schematic illustration of angiotensin II type 1a receptor (AT1aR) biased signaling

591   cascade regulating myogenic arterial tone. Canonical $G_{q/11}$ signaling pathway of the AT1R

592   (purple blue) causes myogenic vasoconstriction whereas noncanonical β-arrestin-biased

593   signaling is not involved in this process. $G_{q/11}$ proteins are heterotrimeric G proteins, which are

594   made up of alpha (α), beta (β) and gamma (γ) subunits. The alpha subunit is attached to

595   either a guanosine triphosphate (GTP) or guanosine diphosphate (GDP), which serves as an

596   on-off switch for the activation of the G-protein. Upon activation of the AT1aR by either

597   ligand-independent mechanical stretch or the natural-biased ligand angiotensin II (Ang II), the

598   Gβγ complex is released from the Gα subunit after its GDP-GTP exchange for canonical G

599   protein signaling to cause myogenic and/or humoral (Ang II-mediated) vasoconstriction. This

600   pathway is inhibited by the $G_{q/11}$ inhibitor FR900359. Although, GRKs and arrestins play a role

601   in multiple noncanonical signaling pathways in cells, this pathway is unlikely engaged by

602   mechanoactivated AT1Rs in response to tensile stretch or their natural ligand angiotensin II to
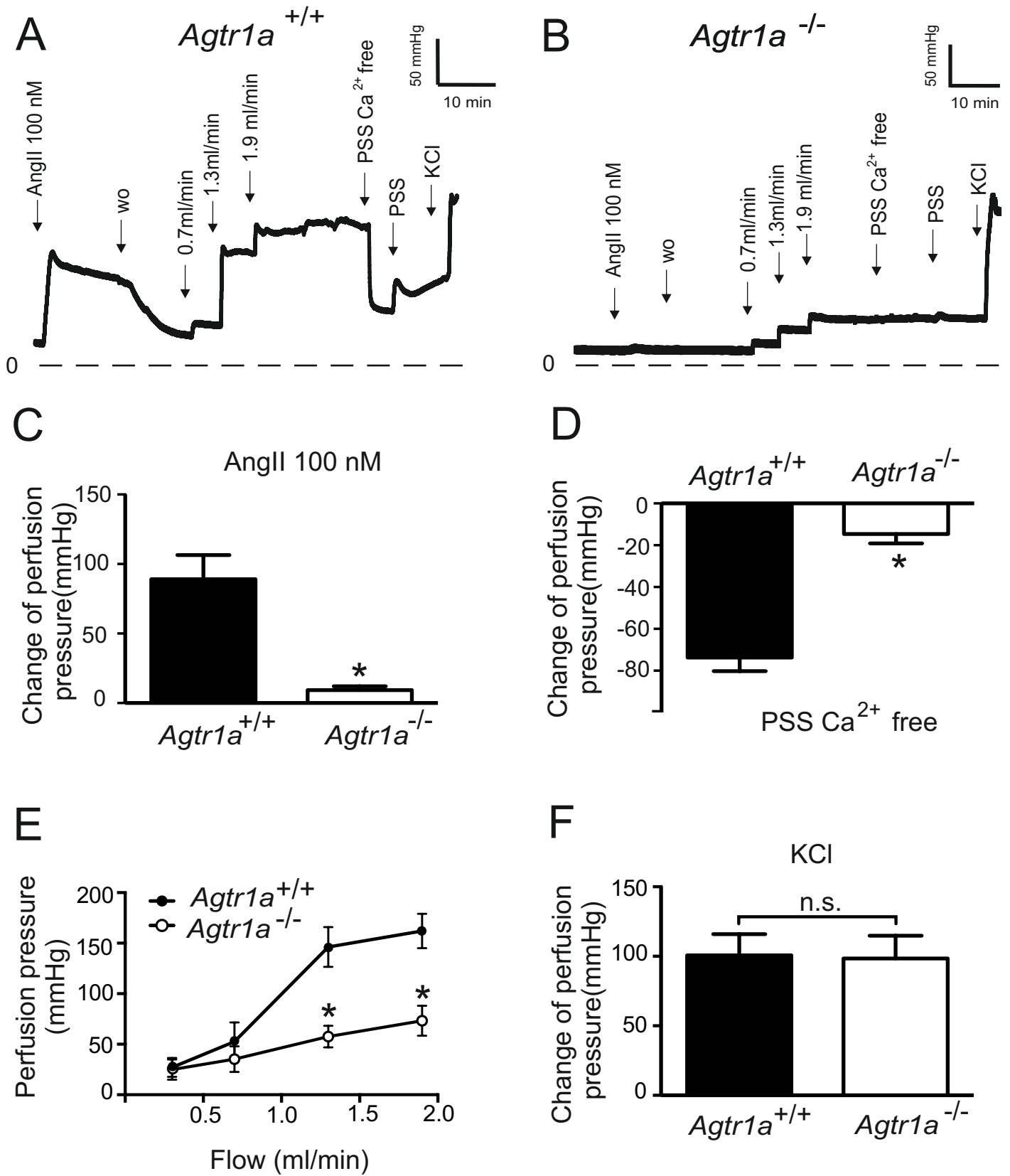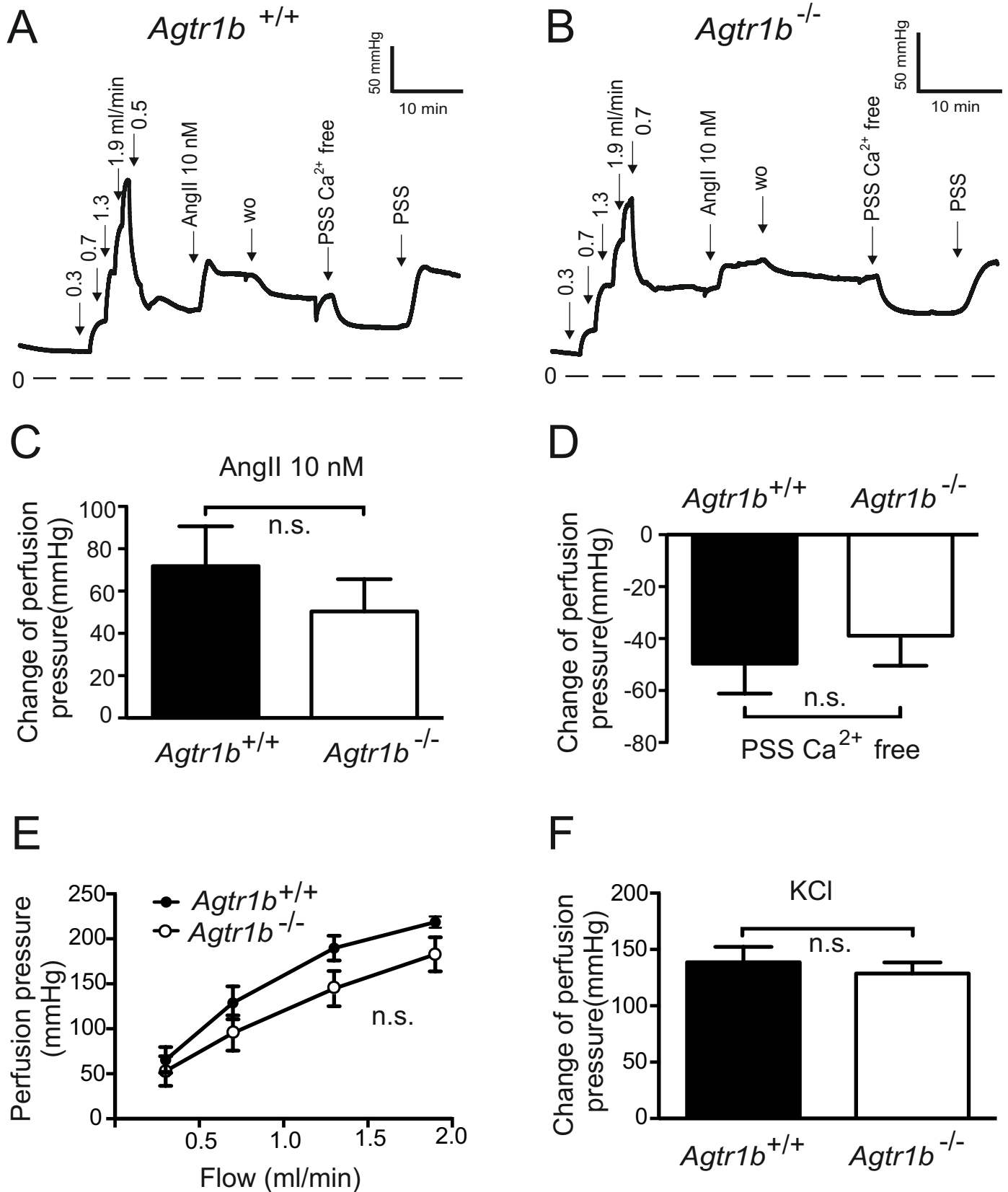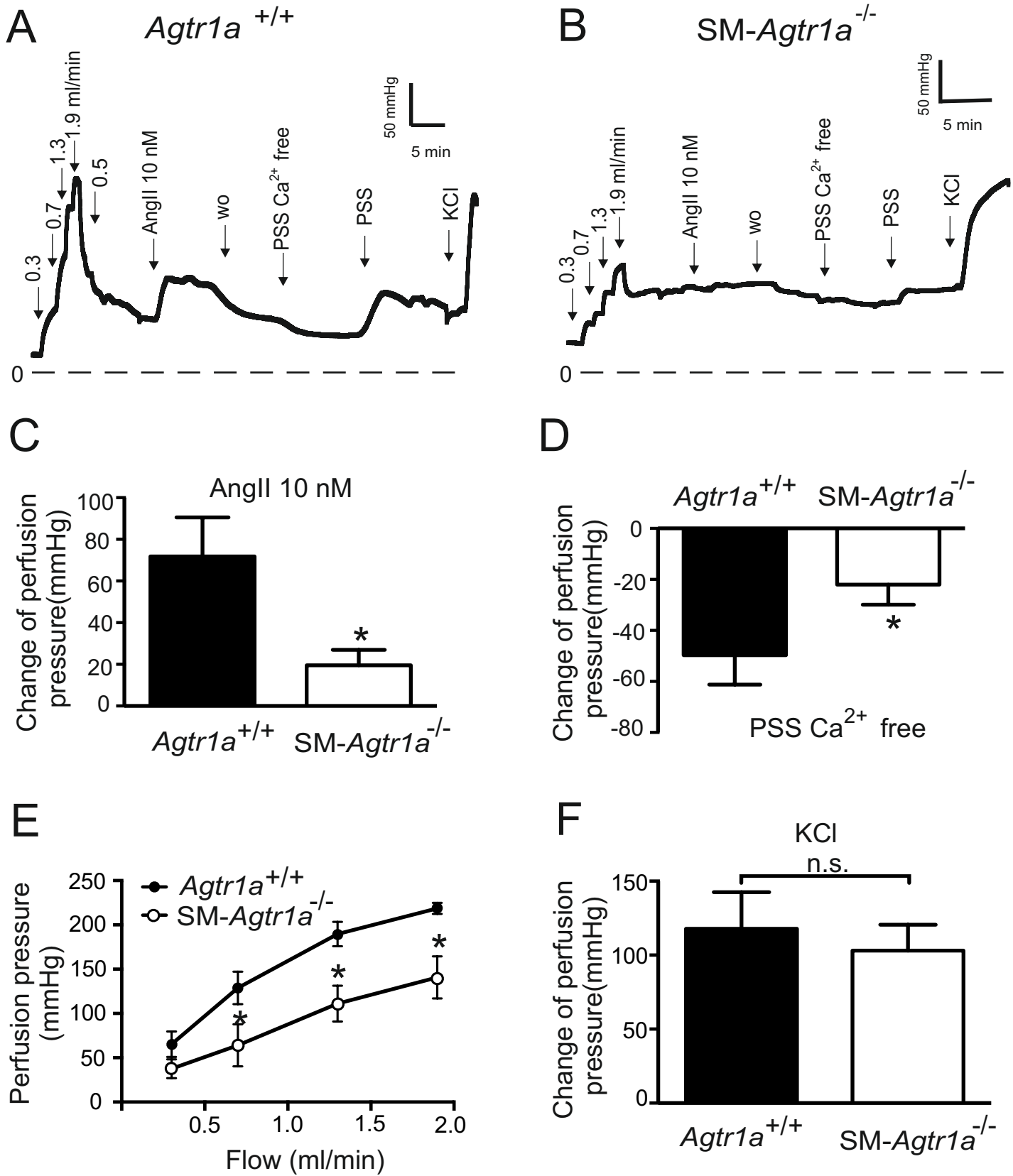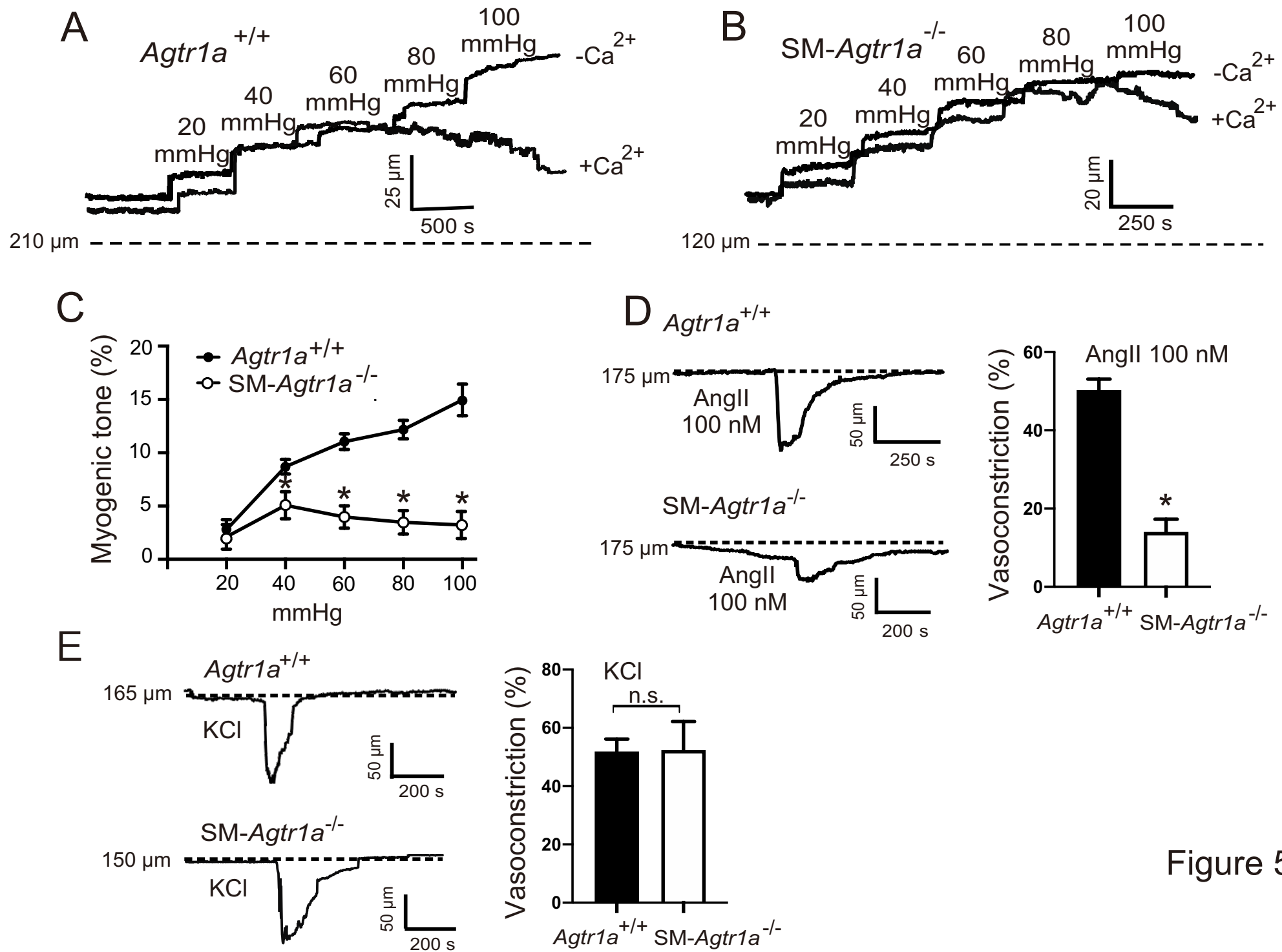
603   cause vasoconstriction.
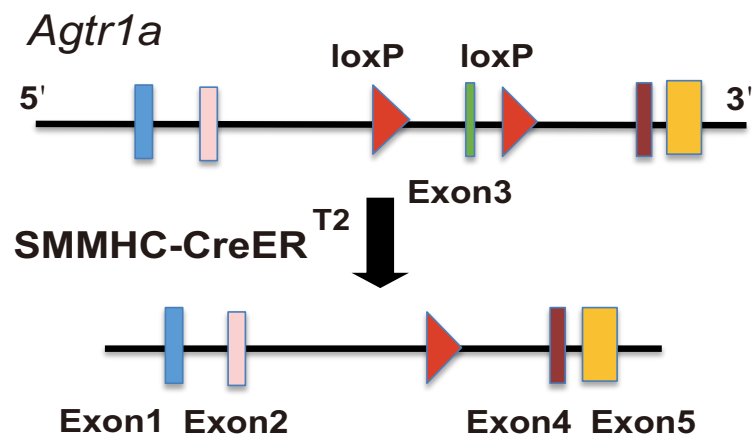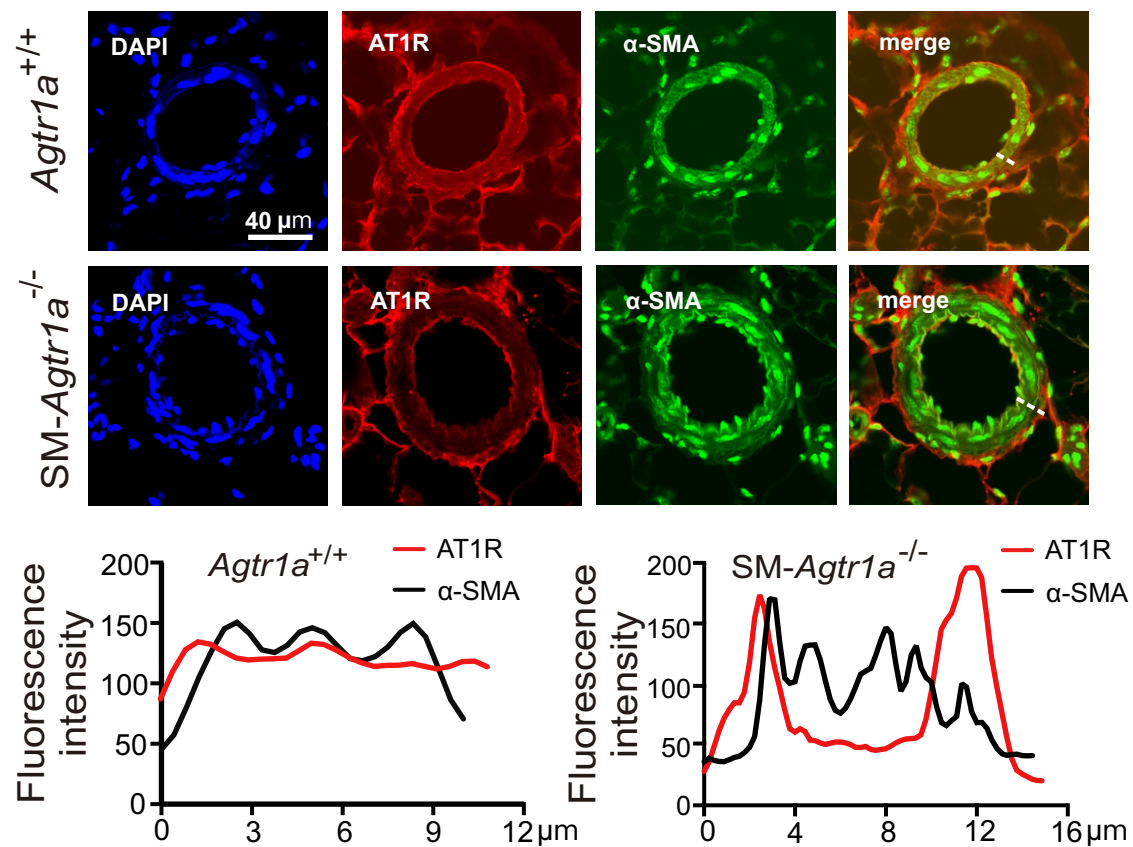
Figure 1

Figure 2

Figure 3

Figure 4

A *Agtr1a*$^{+/+}$

20 mmHg · 40 mmHg · 60 mmHg · 80 mmHg · 100 mmHg

-Ca^{2+}

+Ca^{2+}

25 μm
500 s

210 μm

B SM-*Agtr1a*$^{-/-}$

20 mmHg · 40 mmHg · 60 mmHg · 80 mmHg · 100 mmHg

-Ca^{2+}

+Ca^{2+}

20 μm
250 s

120 μm

C

Myogenic tone (%)

Agtr1a$^{+/+}$
SM-*Agtr1a*$^{-/-}$

mmHg

D *Agtr1a*$^{+/+}$

175 μm

AngII 100 nM

50 μm
250 s

SM-*Agtr1a*$^{-/-}$

175 μm

AngII 100 nM

50 μm
200 s

Vasoconstriction (%)

AngII 100 nM

Agtr1a$^{+/+}$ SM-*Agtr1a*$^{-/-}$

E *Agtr1a*$^{+/+}$

165 μm

KCl

50 μm
200 s

SM-*Agtr1a*$^{-/-}$

150 μm

KCl

50 μm
200 s

Vasoconstriction (%)

KCl

n.s.

Agtr1a$^{+/+}$ SM-*Agtr1a*$^{-/-}$

Figure 5

Figure 6

Figure 7

E

WT

20 mmHg 40 mmHg 60 mmHg 80 mmHg 100 mmHg

$-Ca^{2+}$

+FR900359

$+Ca^{2+}$

25 µm

250 s

75 µm

F

control
FR900359 1 µM

Myogenic tone (%)

mmHg

G

FR900359 1 µM

125 µm

AngII 100 nM

50 µm

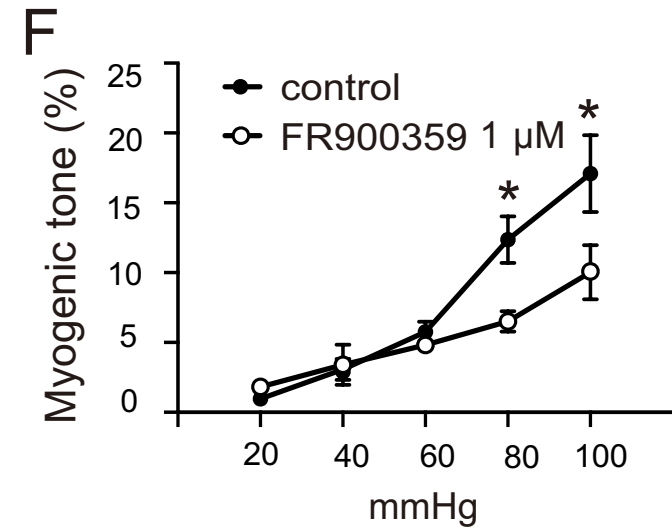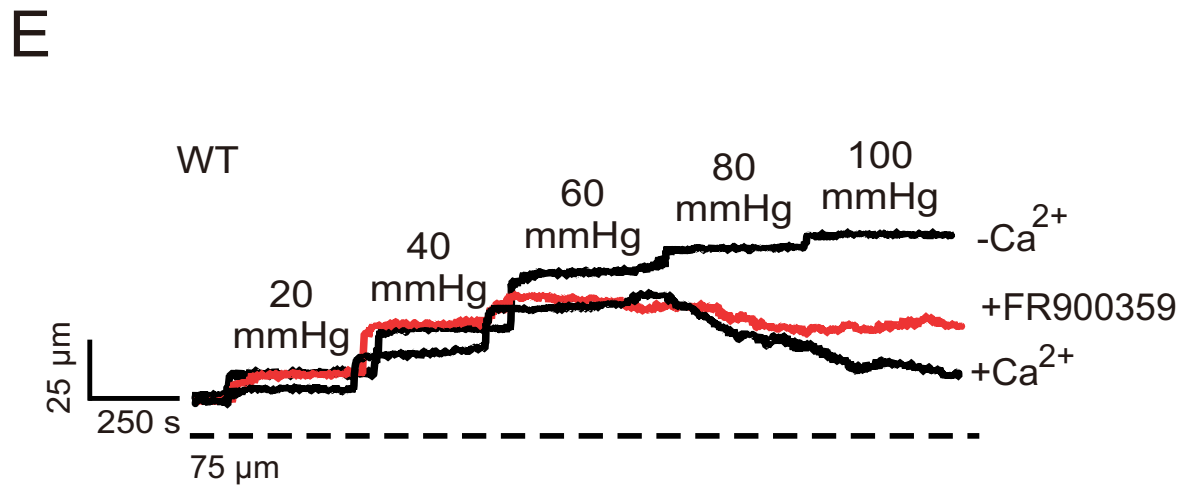100 s

125 µm

AngII 100 nM

50 µm

100 s

H

AngII 100 nM

Vasoconstriction (%)

control   FR900359
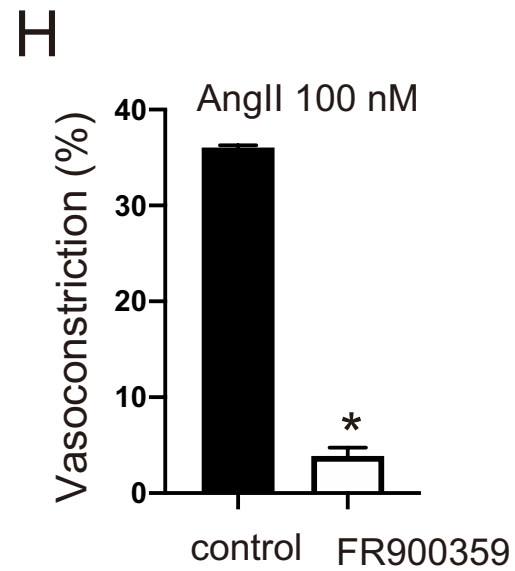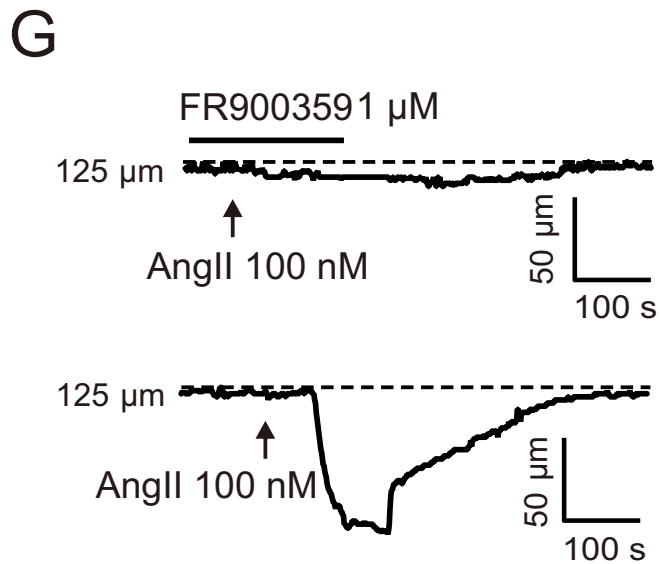
Figure 7

Figure 8

Figure 9